Title

Effects of changing from non-accelerated to accelerated MRI for follow-up in brain atrophy measurement

Authors

Leung, Kelvin K
Malone, Ian M
Ourselin, Sebastien
et al.

Publication Date

2015-02-01

DOI

10.1016/j.neuroimage.2014.11.049

Peer reviewed

Published in final edited form as:
Neuroimage. 2015 February 15; 107: 46–53. doi:10.1016/j.neuroimage.2014.11.049.

Effects of changing from non-accelerated to accelerated MRI for follow-up in brain atrophy measurement

Kelvin K. Leung[a,*], **Ian M. Malone**[a], **Sebastien Ourselin**[a,b], **Jeffrey L. Gunter**[d], **Matt A. Bernstein**[d], **Paul M. Thompson**[c], **Clifford R. Jack Jr.**[d], **Michael W. Weiner**[e], **Nick C. Fox**[a], and **the Alzheimer's Disease Neuroimaging Initiative**[1]

[a]Dementia Research Centre, Department of Neurodegenerative Disease, UCL Institute of Neurology, Queen Square, London WC1N 3BG, UK.

[b]Centre for Medical Image Computing, University College London, WC1E 6BT London, UK.

[c]Departments of Neurology, Psychiatry, Radiology, Engineering, Pediatrics and Ophthalmology, and Imaging Genetics Center, USC Keck School of Medicine, University of Southern California, 2001 N. Soto Street, Los Angeles, CA 90033, USA.

[d]*Mayo Clinic, Rochester, Minnesota, USA.*

[e]Department of Radiology, University of California San Francisco, California ; Magnetic Resonance Imaging Unit, San Francisco Veterans Affairs Hospital San Francisco, California

Abstract

Stable MR acquisition is essential for reliable measurement of brain atrophy in longitudinal studies. One attractive recent advance in MRI is to speed up acquisition using parallel imaging (e.g. reducing volumetric T1-weighted acquisition scan times from around 9 to 5 minutes). In some studies, a decision to change to an accelerated acquisition may have been deliberately taken, while in others repeat scans may occasionally be accidentally acquired with an accelerated acquisition. In ADNI, non-accelerated and accelerated scans were acquired in the same scanning session on each individual. We investigated the impact on brain atrophy as measured by *k*-means normalised boundary shift integral (KN-BSI) and deformation-based morphometry when changing from non-accelerated to accelerated MRI acquisitions over a 12-month interval using scans of 422 subjects from ADNI. KN-BSIs were calculated using both a non-accelerated baseline scan and non-accelerated 12-month scans (i.e. consistent acquisition), and a non-accelerated baseline scan and an accelerated 12-month scan (i.e. changed acquisition). Fluid-based non-rigid registration was also performed on those scans to estimate the brain atrophy rate. We found that the effect on KN-BSI and fluid-based non-rigid registration depended on the scanner manufacturer. For KN-

[*]Corresponding author: Phone: +44 (0)20 3448 4773 kkleung@ucl.ac.uk (Kelvin K. Leung).

[1]Data used in preparation of this article were obtained from the Alzheimers Disease Neuroimaging Initiative (ADNI) database (adni.loni.usc.edu). As such, the investigators within the ADNI contributed to the design and implementation of ADNI and/or provided data but did not participate in analysis or writing of this report. A complete listing of ADNI investigators can be found at: http://adni.loni.usc.edu/wp-content/uploads/how_to_apply/ADNI_Acknowledgement_List.pdf.

BSI, in Philips and Siemens scanners, the change had very little impact on the measured atrophy rate (increase of 0.051% in Philips and -0.035% in Siemens from consistent acquisition to changed acquisition), whereas, in GE, the change caused a mean reduction of 0.65% in the brain atrophy rate. This is likely due to the difference in tissue contrast between grey matter and cerebrospinal fluid in the non-accelerated and accelerated scans in GE, which uses IR-FSPGR instead of MP-RAGE. For fluid-based non-rigid registration, the change caused a mean increase of 0.29% in the brain atrophy rate in the changed acquisition compared to consistent acquisition in Philips, whereas in GE and Siemens, the change had less impact on the mean atrophy rate (increase of 0.18% in GE and 0.049% in Siemens). Moving from non-accelerated baseline scans to accelerated scans for follow-up may have surprisingly little effect on computed atrophy rates depending on the exact sequence details and the scanner manufacturer; even accidentally inconsistent scans of this nature may still be useful.

Keywords

Boundary shift integral; accelerated acquisition; non-accelerated acquisition; brain atrophy; Alzheimer's disease

1. Introduction

Rates of brain atrophy measured from serial MRI are increasingly used to track disease progression for diagnostic purposes and clinical trials (Johnson et al., 2012; Salloway et al., 2014). Stability of acquisition is regarded as absolutely essential (a *sine qua non*) for reliability, with each individual ideally being scanned in the same scanner, using the the same software revision and pulse sequence. This may be impractical for studies of slow-progressing diseases (e.g. Alzheimer's disease) that may go on over 10 years (Bateman et al., 2011). Also, sequence innovations and hardware improvements may mean that there are reasons to change: one attractive recent advance in MRI is to speed up acquisition using parallel imaging methods (reducing volumetric T1-weighted acquisition from approximately 9 to 5 minutes). This frees up scanner time to allow additional scans, or the reduced scan time may reduce patient attrition rate. In some studies, a decision to change to an accelerated acquisition may be beneficial, while in others repeat scans may occasionally be accidentally acquired with an accelerated acquisition.

Popular techniques for the calculation of brain atrophy rate include the boundary shift integral (BSI) (Freeborough and Fox, 1997) and deformation-based morphometry (Freeborough and Fox, 1998; Avants et al., 2008; Hua et al., 2011; Holland et al., 2011; Lorenzi et al., 2013). After registering two serial MR volumetric scans, the BSI directly estimates the change in brain volume using the difference in voxel intensities between the two scans. A change in acquisition protocol (e.g. changing from non-accelerated to accelerated acquisition) is likely to cause a change in image characteristics such as tissue contrast and signal-to-noise ratio, which will have an effect on BSI (Preboske et al., 2006). *K*-means normalised BSI (KN-BSI) can provide a more robust measurement of brain atrophy by using tissue-specific intensity normalisation (Leung et al., 2010). However, KN-BSI still assumes that the tissue intensities in the baseline and repeat scans have a linear

relationship. Deformation-based morphometry uses non-rigid registration to align two serial MR images. Volume change within a region of interests between the two points can be then calculated by integrating the determinant of the Jacobian matrix of the deformation field within the region of interests. Non-rigid registration may be less sensitive to contrast change due to the use of image similarity measures such as normalised cross-correlation and normalised mutual information, but it may be sensitive to the different noise characteristics of the non-accelerated and acceleration scans. We therefore wished to investigate whether KN-BSI and deformation-based morphometry measures would be robust to changing from a non-accelerated acquisition to an accelerated MRI acquisition over a 12-month interval.

2. Materials and Methods

2.1. Image Data and Acquisition

Data used in the preparation of this article were obtained from the Alzheimers Disease Neuroimaging Initiative (ADNI) database (adni.loni.usc.edu). In the second and third phases of ADNI (ADNI-GO and ADNI-2), T1-weighted volumetric MRI scans of each individual were acquired using both non-accelerated and accelerated acquisitions in the same scanning session (IR-FSPGR on GE, and MP-RAGE on Philips and Siemens). The non-accelerated and accelerated MRI protocols are summarised in Table 1. Full details of the MRI protocols are listed on the ADNI website (http://adni.loni.usc.edu/methods/documents/mri-protocols/).

We downloaded the baseline and 1-year non-accelerated and accelerated preprocessed scans of 422 subjects. The subjects consisted of 116 normal controls (NC), 186 subjects with early mild impairment (EMCI), 94 subjects with late mild cognitive impairment (LMCI), and 26 subjects with probable Alzheimer's disease (AD). Image pre-processing included post-acquisition correction of gradient warping (Jovicich et al., 2006) and intensity non-uniformity correction using N3 (Sled et al., 1998) and SPM5 with tissue priors from a custom template consisting of 400 elderly subjects (200 NC and 200 AD) from the first phase of ADNI. A list of subject identifiers used in this study can be found in the supplementary material.

2.2. Brain Atrophy Measurement Using KN-BSI and Deformation-based Morphometry

Whole brain regions in the baseline and repeat scans were automatically delineated by Multi-Atlas Propagation and Segmentation (Leung et al., 2011), visually checked and manually edited if necessary. The baseline and repeat scans were spatially aligned to a mid-point using affine image registration (Leung et al., 2012). Differential bias correction was applied to correct the intensity bias between the aligned scans (Lewis and Fox, 2004).

Brain atrophy rates were then calculated using KN-BSI and deformation-based morphometry.

KN-BSI KN-BSIs (Leung et al., 2010) were calculated using both a non-accelerated baseline scan and non-accelerated repeat scans (i.e. consistent acquisition), and a non-accelerated baseline scan and an accelerated repeat scan (i.e. changed acquisition). Brain atrophy rate was calculated as a percentage of the baseline brain volume by dividing the KN-BSI by the baseline brain volume.

Deformation-based Morphometry Fluid-based non-rigid registration (Freeborough and Fox, 1998; Anderson et al., 2012) was used to register a non-accelerated baseline scan and non-accelerated repeat scans (i.e. consistent acquisition), and a non-accelerated baseline scan and an accelerated repeat scan (i.e. changed acquisition). Normalised cross-correlation was used as the similarity measure in the registration. Brain volume change was calculated by integrating the determinant of the Jacobian matrix of the deformation field within the baseline whole brain region. Brain atrophy rate was calculated as a percentage of the baseline brain volume by dividing the brain volume change by the baseline brain volume.

2.3. Tissue Contrast

As a change of tissue contrast between the baseline and repeat scans may cause a change in KN-BSI, we obtained the mean intensities of cerebrospinal fluid (CSF), grey matter (GM) and white matter (WM) in the non-accelerated and accelerated scans using *k*-means clustering (in the KN-BSI pipeline) (Leung et al., 2010), and calculated GM-CSF and WM-GM tissue contrast ratios.

2.4. Statistical Analysis

Linear regression was used to compare the measured brain atrophy rates between consistent and changed acquisitions for each manufacturer with the site ID as a covariate, and to compare the log-transformed GMCSF and WM-GM ratios between non-accelerated and accelerated scans. In addition, Pitman's test was used to compare the variances of measured brain atrophy rates between consistent and changed acquisitions for each manufacturer. All statistical analyses were performed using Stata version 12.1 (College Station, Texas, US).

3. Results

Figure 1 shows examples of non-accelerated and accelerated scans from each manufacturer. The non-accelerated and accelerated scans were qualitatively very similar, with some subtle differences in terms of noise characteristics. Table 2 shows the brain atrophy rates calculated from KN-BSI using consistent and changed acquisitions. Mean atrophy rates from the changed acquisition were 0.65% (95% CI [0.39%, 0.91%], $p<0.001$) lower than the consistent acquisition in GE. There was no evidence that the mean atrophy rates from the changed and consistent acquisitions were different ($p>0.6$, both tests) in Philips and Siemens. Similar patterns were observed in each diagnosis (see also Figure 2). We did not find any statistically significant differences ($p>0.4$, all tests) in the variances of the measured atrophy rates between consistent acquisition and changed acquisition for each manufacturer. As shown in Figure 3, the variability in sites with Philips scanners appears to be lower than Siemens and GE. In addition, we found that the GM-CSF ratio between the non-accelerated and accelerated scans in GE had a difference of 6.3% ($p<0.001$) (see Table 3). The GM-CSF and WM-GM ratios between non-accelerated and accelerated scans in Philips and Siemens were less than 1%.

Table 4 shows the brain atrophy rates calculated from fluid-based non-rigid registration using consistent and changed acquisitions. Mean atrophy rates from the changed acquisition were 0.29% (95% CI [0.11%, 0.47%], $p=0.002$) higher than the consistent acquisition in

Philips. There was no evidence that the mean atrophy rates from the changed and consistent acquisitions were different ($p>0.4$, both tests) in GE and Siemens. Similar patterns were observed in each diagnosis (see also Figure 4).

3.1. Posthoc analysis

The results so far suggested that the effect on the atrophy rate estimated by KN-BSI in GE might be due to the difference in GM-CSF ratio between the non-accelerated and accelerated scans in GE. In this posthoc analysis, we modified the intensity normalisation procedure in KN-BSI. In Leung et al. (2010), the intensity of the repeat scans was mapped to the baseline scans (and vice versa) using simple linear regression (mean CSF, GM, WM and whole brain intensities as data points). Here, we replaced it by piece-wise linear regression (mean CSF, GM and WM intensities as data points) (Nyúl and Udupa, 1999), in order to model the non-linear tissue contrast change. In the piece-wise linear regression, the intensity range of the baseline and repeat scans were divided into two sections by the mean GM intensity. For the voxels with intensity lower than mean GM intensity, the mean CSF and GM intensities were used to perform the linear regression and intensity normalisation. Likewise, for the voxels with intensity higher than mean GM intensity, the mean GM and WM intensities were used to perform the linear regression and intensity normalisation.

Table 5 shows the brain atrophy rates (% baseline volume) calculated from baseline and 12-month scans when using piece-wise linear regression (instead of simple linear regression) in the intensity normalisation procedure in KN-BSI. Mean atrophy rates from the changed acquisition were 0.40% (95% CI [0.15%, 0.65%], $p=0.002$) lower than the consistent acquisition in GE. Compared to table 2, using piece-wise linear regression can reduce the difference between the brain atrophy rate calculated using consistent and changed acquisitions in GE.

4. Conclusions and Discussion

We found that the effect on KN-BSI and fluid-based non-rigid registration when changing from non-accelerated to accelerated MRI during follow-up depended on the scanner manufacturer. For KN-BSI, the change caused a mean reduction of 0.65% in the brain atrophy rate in GE, whereas in Philips and Siemens, the change had little impact on the mean atrophy rate (reduction of 0.051% in Philips and -0.035% in Siemens). The effect on the atrophy rate estimated by KN-BSI in GE is likely due to the difference in GM-CSF ratio between the non-accelerated and accelerated scans in GE (6.3% difference between non-accelerated and accelerated scans). This is because KN-BSI assumes that the intensities of different tissues in the baseline and repeat scans have a linear relationship, and in this case, the GM-CSF ratio between the non-accelerated and accelerated scans in GE changed while the WM-GM ratio remained similar. Although WM-GM ratio changes significantly ($p=0.004$) for Philips, the difference is relatively small (0.7% difference between the non-accelerated and accelerated scans - an order of magnitude smaller than GE). When using piece-wise linear regression instead of simple linear regression, in the intensity normalisation in KN-BSI, the difference between the mean atrophy rates between consistent and changed acquisitions in GE was reduced to 0.40% from 0.65%.

For fluid-based non-rigid registration, the change caused a mean increase of 0.29% in the brain atrophy rate in the changed acquisition compared to consistent acquisition in Philips, whereas in GE and Siemens, the change had less impact on the mean atrophy rate (increase of 0.18% in GE and 0.049% in Siemens). As normalised cross correlation was used in the fluid-based registration, it was not affected by the tissue contrast change in GE. Since the fluid-based non-rigid registration is sensitive to the level of noise in the baseline and repeat scans, the brain atrophy reduction may be caused by different noise characteristics in the non-accelerated and accelerated scans.

Across different sites with the same scanner vendor, the effect on KN-BSI when changing from non-accelerated to accelerated MRI during follow-up showed minor differences. The variability in sites with Philips scanners appear to be more consistent than Siemens and GE.

A change in tissue contrast between the baseline and repeat has been shown to affect BSI (Preboske et al., 2006). Switching from a conventional SPGR to a fast SPGR sequence caused a change of 0.43% in BSI (the fast SPGR acquired a fractional echo which in turn exacerbates local susceptibility artifacts, and used a different implementation of spoiler gradients). In addition, changing the flip angle in the repeat scan from 25° to 12° and 5° caused a change of 1.85% and 30.45% in BSI (relative to the BSI using the flip angle of 25° in both baseline and repeat scans). Consistent acquisition is crucial for atrophy rate measurement using BSI and KN-BSI.

Another related study compared brain atrophy rates (using a similar pipeline to KN-BSI) of consistent acquisitions with different acceleration factors and head coil types in a Siemens scanner (Krueger et al., 2012). Brain atrophy rates of consistent accelerated acquisitions with an acceleration factor less than 5 were found to be similar. However, a systematic difference of 0.5% was observed in whole-brain BSI between consistent acquisitions using 32- and 12-channel coils, and the authors stated that it could arise from differences in repositioning and shims after the coil change during the scanning session.

The difference in tissue contrast between non-accelerated and accelerated scans in GE does not appear to be caused by the reconstruction algorithm. Philips uses SENSE recontruction (Pruessmann et al., 1999) and GE uses the closely related ASSET method, while Siemens uses GRAPPA recontruction (Griswold et al., 2002). The difference also does not appear to relate to the looping order of the phase-encoded views, because both GE and Siemens encode ky in the outer loop and kz in the inner loop while Philips does the opposite. Similarly, as the pixel size between the accelerated and non-accelerated acquisitions is most different in Philips, the slight variation in pixel size between the accelerated and non-accelerated acquisitions does not seem to be the source of the variation. The accelerated scans are acquired with slightly larger pixels to partially compensate for the SNR reduction associated with parallel imaging, which can be needed unless a 32-channel head coil is used (Krueger et al., 2012). Note, however, from Table 1 that the GE pixel size change is intermediate between Siemens and Philips. Eliminating these varying factors suggests to us that the difference in acquisition technique (IR-FSPGR vs. MP-RAGE) is the primary source of the observed difference in BSI measures, although our analysis of the ADNI data in this

study does not demonstrate this directly, as there are other software and hardware differences between the scanners from different vendors.

Previous studies have compared atrophy rates calculated from consistent non-accelerated acquisition and consistent accelerated acquisition (Ching et al., 2012, 2014). The authors estimated atrophy rates from ADNI scans using tensor-based morphometry. They found that the estimated atrophy rates from consistent non-accelerated acquisition and consistent accelerated acquisition were very similar, and that they had similar power to track brain changes. We are not aware of any previous study comparing atrophy rates calculated from consistent and changed acquisitions.

The current study only investigated the effects on KN-BSI of changing from non-accelerated to accelerated MRI in repeat scans in brain atrophy measurement. And we only used the non-accelerated and accelerated MP-RAGE/IR-SPGR scans acquired from GE, Philips and Siemens scanners. The difference in atrophy rate between consistent and changed acquisition did not appear to depend on the diagnosis of the subjects, although only a small number of AD subjects in ADNI was available at the time of the study. Furthermore, similar analysis should be repeated in a different study to investigate the generality of the results and conclusions.

A strong point of the current study is the relatively large number of subjects provided by ADNI. Also, ADNI is a multi-centre study, and the accelerated and non-accelerated scans were acquired on the same scanning session for all the subjects.

Going from non-accelerated baseline scans to accelerated scans for follow-up may have surprisingly little effect on computed atrophy rates depending on the exact sequence details and the scanner manufacturer, so that accidentally inconsistent scans of this nature could still be used.

Supplementary Material

Refer to Web version on PubMed Central for supplementary material.

Acknowledgements

The ADNI was launched in 2003 by the National Institute on Aging (NIA), the National Institute of Biomedical Imaging and Bioengineering (NIBIB), the Food and Drug Administration (FDA), private pharmaceutical companies and non-profit organizations, as a $60 million, 5-year public-private partnership. The primary goal of ADNI has been to test whether serial magnetic resonance imaging (MRI), positron emission tomography (PET), other biological markers, and clinical and neuropsychological assessment can be combined to measure the progression of mild cognitive impairment (MCI) and early Alzheimers disease (AD). Determination of sensitive and specific markers of very early AD progression is intended to aid researchers and clinicians to develop new treatments and monitor their effectiveness, as well as lessen the time and cost of clinical trials. The Principal Investigator of this initiative is Michael W. Weiner, MD, VA Medical Center and University of California San Francisco. ADNI is the result of efforts of many co-investigators from a broad range of academic institutions and private corporations, and subjects have been recruited from over 50 sites across the U.S. and Canada. The initial goal of ADNI was to recruit 800 subjects but ADNI has been followed by ADNI-GO and ADNI-2. To date these three protocols have recruited over 1500 adults, ages 55 to 90, to participate in the research, consisting of cognitively normal older individuals, people with early or late MCI, and people with early AD. The follow up duration of each group is specified in the protocols for ADNI-1, ADNI-2 and ADNI-GO. Subjects originally recruited for ADNI-1 and ADNI-GO had the option to be followed in ADNI-2. For up-to-date information, see www.adni-info.org.

Data collection and sharing for this project was funded by the Alzheimer's Disease Neuroimaging Initiative (ADNI) (National Institutes of Health Grant U01 AG024904) and DOD ADNI (Department of Defense award number W81XWH-12-2-0012). ADNI is funded by the National Institute on Aging, the National Institute of Biomedical Imaging and Bioengineering, and through generous contributions from the following: Alzheimers Association; Alzheimers Drug Discovery Foundation; BioClinica, Inc.; Biogen Idec Inc.; Bristol-Myers Squibb Company; Eisai Inc.; Elan Pharmaceuticals, Inc.; Eli Lilly and Company; F. Hoffmann-La Roche Ltd and its affiliated company Genentech, Inc.; GE Healthcare; Innogenetics, N.V.; IXICO Ltd.; Janssen Alzheimer Immunotherapy Research & Development, LLC.; Johnson & Johnson Pharmaceutical Research & Development LLC.; Medpace, Inc.; Merck & Co., Inc.; Meso Scale Diagnostics, LLC.; NeuroRx Research; Novartis Pharmaceuticals Corporation; Pfizer Inc.; Piramal Imaging; Servier; Synarc Inc.; and Takeda Pharmaceutical Company. The Canadian Institutes of Health Research is providing funds to Rev December 5, 2013 support ADNI clinical sites in Canada. Private sector contributions are facilitated by the Foundation for the National Institutes of Health (www.fnih.org). The grantee organization is the Northern California Institute for Research and Education, and the study is coordinated by the Alzheimer's Disease Cooperative Study at the University of California, San Diego. ADNI data are disseminated by the Laboratory for Neuro Imaging at the University of Southern California.

The Dementia Research Centre is supported by Alzheimer's Research UK, Brain Research Trust, and The Wolfson Foundation. KKL is supported by ADNI. NCF has an NIHR Senior Investigator award and receives support from the Wolfson Foundation; the NIHR Biomedical Research Unit (Dementia) at UCL; the EPSRC and Alzheimers Research UK.

The authors would like to thank the image analysts and the research associates in the Dementia Research Centre for their help in the study, and the ADNI study subjects and investigators for their participation.

References

Anderson VM, Schott JM, Bartlett JW, Leung KK, Miller DH, Fox NC. Gray matter atrophy rate as a marker of disease progression in ad. Neurobiol Aging. Jul; 2012 33(7):1194–1202. URL http://dx.doi.org/10.1016/j.neurobiolaging.2010.11.001. [PubMed: 21163551]

Avants BB, Epstein CL, Grossman M, Gee JC. Symmetric diffeomorphic image registration with cross-correlation: evaluating automated labeling of elderly and neurodegenerative brain. Med Image Anal. Feb; 2008 12(1):26–41. [PubMed: 17659998]

Bateman R, Aisen P, De Strooper B, Fox N, Lemere C, Ringman J, Salloway S, Sperling R, Windisch M, Xiong C. Autosomal-dominant alzheimer's disease: a review and proposal for the prevention of alzheimer's disease. Alzheimer's Research & Therapy. 2011; 3(1):1.

Ching, CRK.; Hua, X.; Hibar, DP.; Ward, CP.; Gunter, JL.; Bernstein, MA.; C. R. J.; Weiner, MW.; the Alzheimers Disease Neuroimaging Initiative. P. M. T.. MRI scan acceleration and power to track brain change. MICCAI NIBAD; 2012.

Ching CRK, Hua X, Hibar DP, Ward CP, Gunter JL, Bernstein MA, C. R. J. Weiner MW, Thompson PM, the Alzheimers Disease Neuroimaging Initiative. Does MRI scan acceleration affect power to track brain change? Neurobiology of Aging in press. Apr.2014

Freeborough P, Fox N. The boundary shift integral: an accurate and robust measure of cerebral volume changes from registered repeat MRI. IEEE Transactions in Medical Imaging. 1997; 16(5):623–629.

Freeborough PA, Fox NC. Modeling brain deformations in Alzheimer disease by fluid registration of serial 3D MR images. J Comput Assist Tomogr. 1998; 22(5):838–843. [PubMed: 9754126]

Griswold MA, Jakob PM, Heidemann RM, Nittka M, Jellus V, Wang J, Kiefer B, Haase A. Generalized autocalibrating partially parallel acquisitions (GRAPPA). Magn Reson Med. Jun; 2002 47(6):1202–1210. [PubMed: 12111967]

Holland D, Dale AM, A. D. N. I. Nonlinear registration of longitudinal images and measurement of change in regions of interest. Med Image Anal. Aug; 2011 15(4):489–497. [PubMed: 21388857]

Hua X, Gutman B, Boyle CP, Rajagopalan P, Leow AD, Yanovsky I, Kumar AR, Toga AW, Jack CR, Schuff N, Alexander GE, Chen K, Reiman EM, Weiner MW, Thompson PM, the Alzheimer's Disease Neuroimaging Initiative. Accurate measurement of brain changes in longitudinal MRI scans using tensor-based morphometry. NeuroImage. Jul; 2011 57(1):5–14. [PubMed: 21320612]

Johnson KA, Fox NC, Sperling RA, Klunk WE. Brain imaging in alzheimer disease. Cold Spring Harbor perspectives in medicine. 2012; 2(4):a006213. [PubMed: 22474610]

Jovicich J, Czanner S, Greve D, Haley E, van der Kouwe A, Gollub R, Kennedy D, Schmitt F, Brown G, Macfall J, Fischl B, Dale A. Reliability in multi-site structural MRI studies: effects of gradient

non-linearity correction on phantom and human data. Neuroimage. Apr; 2006 30(2):436–443. [PubMed: 16300968]

Krueger G, Granziera C, Jack CR, Gunter JL, Littmann A, Mortamet B, Kannengiesser S, Sorensen AG, Ward CP, Reyes DA, Britson PJ, Fischer H, Bernstein MA. Effects of mri scan acceleration on brain volume measurement consistency. Journal of Magnetic Resonance Imaging. 2012; 36(5): 1234–1240. [PubMed: 22570196]

Leung KK, Barnes J, Modat M, Ridgway GR, Bartlett JW, Fox NC, Ourselin S, Alzheimer's Disease Neuroimaging Initiative. Brain MAPS: An automated, accurate and robust brain extraction technique using a template library. NeuroImage. Apr; 2011 55(3):1091–1108. [PubMed: 21195780]

Leung KK, Clarkson MJ, Bartlett JW, Clegg S, Jack CR, Weiner MW, Fox NC, Ourselin S, Alzheimer's Disease Neuroimaging Initiative. Robust atrophy rate measurement in Alzheimer's disease using multi-site serial MRI: tissue-specific intensity normalization and parameter selection. NeuroImage. Apr; 2010 50(2):516–523. [PubMed: 20034579]

Leung KK, Ridgway GR, Ourselin S, Fox NC. Consistent multi-time-point brain atrophy estimation from the boundary shift integral. NeuroImage. 2012; 59(4):3995–4005. [PubMed: 22056457]

Lewis EB, Fox NC. Correction of differential intensity inhomogeneity in longitudinal MR images. NeuroImage. 2004; 23(1):75–83. [PubMed: 15325354]

Lorenzi M, Ayache N, Frisoni GB, Pennec X, A. D. N. I. A. D. N. I. Lcc-demons: a robust and accurate symmetric diffeomorphic registration algorithm. Neuroimage. Nov.2013 81:470–483. [PubMed: 23685032]

Nyúl LG, Udupa JK. On standardizing the MR image intensity scale. Magn Reson Med. Dec; 1999 42(6):1072–1081. [PubMed: 10571928]

Preboske GM, Gunter JL, Ward CP, Jack CR. Common MRI acquisition non-idealities significantly impact the output of the boundary shift integral method of measuring brain atrophy on serial MRI. NeuroImage. May; 2006 30(4):1196–1202. [PubMed: 16380273]

Pruessmann KP, Weiger M, Scheidegger MB, Boesiger P. SENSE: sensitivity encoding for fast MRI. Magn Reson Med. Nov; 1999 42(5):952–962. [PubMed: 10542355]

Salloway S, Sperling R, Fox NC, Blennow K, Klunk W, Raskind M, Sabbagh M, Honig LS, Porsteinsson AP, Ferris S, Reichert M, Ketter N, Nejadnik B, Guenzler V, Miloslavsky M, Wang D, Lu Y, Lull J, Tudor IC, Liu E, Grundman M, Yuen E, Black R, Brashear HR. Two phase 3 trials of bapineuzumab in mild-to-moderate alzheimer's disease. New England Journal of Medicine. 2014; 370(4):322–333. [PubMed: 24450891]

Sled JG, Zijdenbos AP, Evans AC. A nonparametric method for automatic correction of intensity nonuniformity in MRI data. IEEE Trans Med Imaging. Feb; 1998 17(1):87–97. [PubMed: 9617910]

Highlights

Repeat scans may accidently be acquired with accelerated instead of non-accelerated acquisition.

We study the impact on atrophy rate when going from non-accelerated to accelerated acquisitions

Little impact on KN-BSI in Philips and Siemens scanners, but mean reduction of 0.65% in GE

Little impact on non-rigid registration in GE and Siemens, but mean increase of 0.29% in Philips

Moving from non-accelerated scans to accelerated scans may have surprisingly little effect

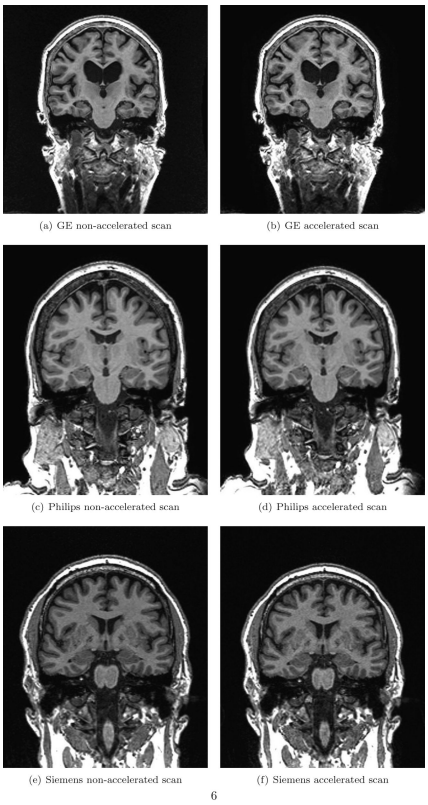

Figure 1.
Examples of non-accelerated and accelerated scans from each manufacturer.

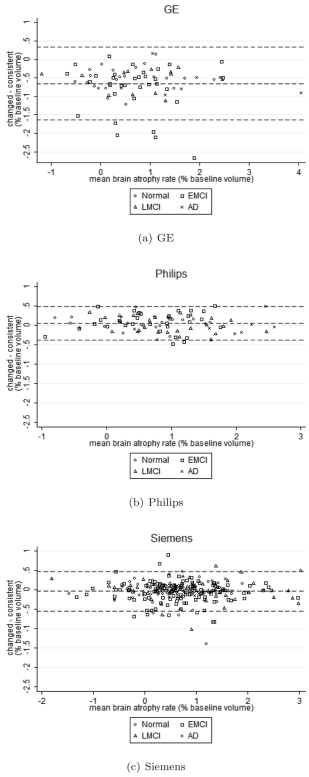

Figure 2.

Bland-Altman plots of the difference in brain atrophy rate between the consistent and changed acquisition using KN-BSI. The dotted lines show the mean and mean±1.96*SD of the difference.

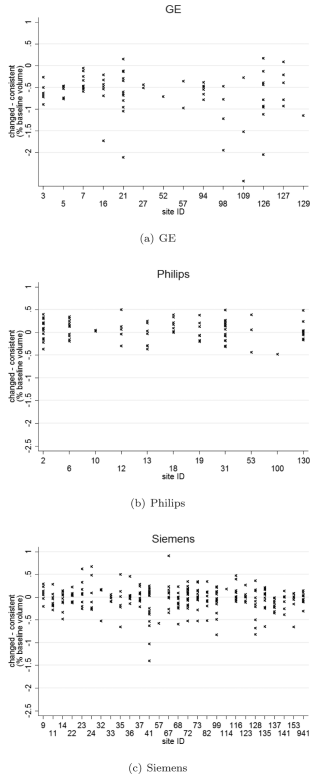

Figure 3.

Difference in brain atrophy rate between the consistent and changed acquisitions using KN-BSI against site ID.

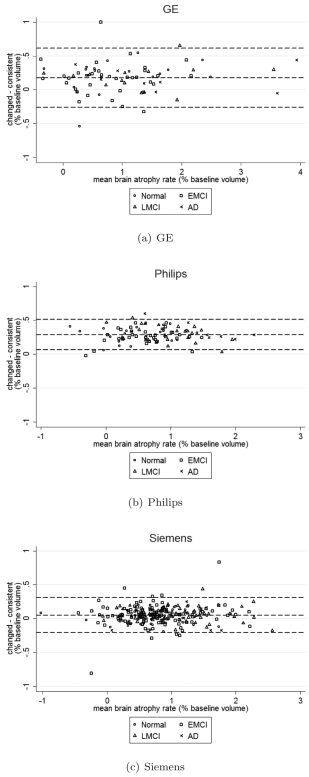

Figure 4.

Bland-Altman plots of the difference in brain atrophy rate between the consistent and changed acquisition using fluid-based non-rigid registration. The dotted lines show the mean and mean±1.96*SD of the difference.

Table 1

Summary of non-accelerated and accelerated MRI protocols for T1-weighted scans in ADNI-GO and ADNI-2.

Manufacturer		TR/MPRAGE TR (ms)	TE (ms)	TI (ms)	Flip angle (°)	Slice thickness (mm)	Acquired pixel dimensions (mm)	Scan time (min:sec)
GE	Non-accelerated	7.0 –7.7/na	2.8 – 3.2	400	11	1.20	1.02 × 1.02	9:41
	Accelerated	7.0 –7.7/na	2.8 – 3.2	400	11	1.20	1.05 × 1.05	5:34
Philips	Non-accelerated	6.8/2500	3.1	900	9	1.20	1.00 × 1.00	9:07
	Accelerated	6.8/2500	3.1	900	9	1.20	1.11 × 1.11	5:34
Siemens	Non-accelerated	7.1/2300	3.0	900	9	1.20	1.00 × 1.00	9:14
	Accelerated	7.0/2300	3.0	900	9	1.20	1.05 × 1.05	5:12

Table 2

Mean (SD) brain atrophy rate (% baseline volume) calculated from baseline and 12-month scans using KN-BSI, and the difference [95% CI] in mean brain atrophy rate between the consistent and changed acquisitions.

Manufacturer		Consistent acquisition (baseline non-accelerated and repeat non-accelerated scans)	Changed acquisition (baseline non-accelerated and repeat accelerated scans)	Difference (changed - consistent)
GE	**All (n=76)**	**1.099 (0.924)**	**0.449 (0.897)**	**−0.650 [−0.940, −0.360], p<0.001***
	NC (n=20)	0.841 (0.897)	0.341 (0.759)	−0.500 [−0.985, −0.015], p=0.04*
	EMCI (n=34)	1.093 (0.841)	0.314 (0.779)	−0.780 [−1.160, −0.399], p<0.001*
	LMCI (n=14)	1.020 (0.956)	0.456 (0.955)	−0.565 [−1.232, 0.102], p=0.09
	AD (n=8)	1.901 (1.308)	1.280 (1.261)	−0.621 [−1.293, 0.051], p=0.07
Philips	**All (n=90)**	**0.800 (0.754)**	**0.852 (0.736)**	**0.051 [−0.173, 0.276], p=0.7**
	NC (n=25)	0.510 (0.652)	0.563 (0.637)	0.054 [−0.316, 0.423], p=0.8
	EMCI (n=34)	0.663 (0.628)	0.754 (0.656)	0.091 [−0.220, 0.403], p=0.6
	LMCI (n=24)	0.974 (0.734)	0.983 (0.663)	0.010 [−0.372, 0.391], p>0.9
	AD (n=7)	1.910 (0.696)	1.903 (0.776)	−0.007 [−0.917, 0.902], p>0.9
Siemens	**All (n=256)**	**0.729 (0.793)**	**0.694 (0.787)**	**−0.035 [−0.170, 0.101], p=0.6**
	NC (n=71)	0.587 (0.629)	0.551 (0.623)	−0.035 [−0.225, 0.154], p=0.7
	EMCI (n=118)	0.678 (0.779)	0.623 (0.767)	−0.055 [−0.242, 0.133], p=0.6
	LMCI (n=56)	0.958 (0.972)	0.951 (0.952)	−0.006 [−0.332, 0.320], p>0.9
	AD (n=11)	1.036 (0.651)	1.075 (0.691)	0.0394 [−0.526, 0.605], p=0.9

*Results with $p < 0.05$ are marked with.

Table 3

Geometric means [95% CI] of the tissue contrast ratios and their differences (in terms of ratio).

Manufacturer		Non-accelerated	Accelerated	Difference (non-accelerated/ accelerated)
GE (n=76)	GM-CSF ratio	2.607 [2.565, 2.649]	2.452 [2.417, 2.488]	1.063 [1.040, 1.089], p<0.001*
	WM-GM ratio	1.459 [1.451, 1.466]	1.446 [1.439, 1.454]	1.008 [1.001, 1.016], p=0.02*
Philips (n=90)	GM-CSF ratio	2.343 [2.320, 2.367]	2.322 [2.298, 2.347]	1.009 [0.995, 1.024], p=0.2
	WM-GM ratio	1.408 [1.404, 1.413]	1.398 [1.394, 1.403]	1.007 [1.002, 1.012], p=0.004*
Siemens (n=256)	GM-CSF ratio	2.411 [2.396, 2.427]	2.407 [2.392, 2.422]	1.002 [0.993, 1.011], p=0.7
	WM-GM ratio	1.436 [1.433, 1.439]	1.434 [1.431, 1.437]	1.001 [0.998, 1.004], p=0.4

*Results with $p < 0.05$ are marked with. CSF: cerebrospinal fluid, GM: grey matter, and WM: white matter.

Table 4

Mean (SD) brain atrophy rate (% baseline volume) calculated from baseline and 12-month scans using fluid-based non-rigid registration, and the difference [95% CI] in mean brain atrophy rate between the consistent and changed acquisitions.

Manufacturer		Consistent acquisition (baseline non-accelerated and repeat non-accelerated scans)	Changed acquisition (baseline non-accelerated and repeat accelerated scans)	Difference (changed - consistent)
GE	**All (n=76)**	**0.921 (0.857)**	**1.098 (0.876)**	**0.177 [0.101, 0.455], p=0.2**
	NC (n=20)	0.760 (0.724)	0.965 (0.794)	0.205 [−0.300, 0.710], p=0.4
	EMCI (n=34)	0.735 (0.640)	0.897 (0.642)	0.163 [−0.132, 0.457], p=0.3
	LMCI (n=14)	1.187 (0.947)	1.363 (0.978)	0.177 [−0.432, 0.785], p=0.6
	AD (n=8)	1.650 (1.360)	1.812 (1.345)	0.170 [−0.890, 1.229], p=0.7
Philips	**All (n=90)**	**0.614 (0.5537)**	**0.904 (0.552)**	**0.290 [0.123, 0.456], p=0.001***
	NC (n=25)	0.383 (0.491)	0.686 (0.508)	0.303 [0.007, 0.599], p=0.05*
	EMCI (n=34)	0.492 (0.424)	0.751 (0.441)	0.259 [0.045, 0.473], p=0.02*
	LMCI (n=24)	0.796 (0.523)	1.101 (0.473)	0.305 [0.047, 0.563], p=0.02*
	AD (n=7)	1.413 (0.605)	1.751 (0.483)	0.338 [−0.252, 0.928], p=0.5
Siemens	**All (n=256)**	**0.803 (0.543)**	**0.852 (0.555)**	**0.048 [− 0.045, 0.142], p=0.4**
	NC (n=71)	0.674 (0.449)	0.712 (0.464)	0.038 [−0.094, 0.170], p=0.6
	EMCI (n=118)	0.750 (0.526)	0.802 (0.544)	0.051 [−0.075, 0.178], p=0.4
	LMCI (n=56)	1.016 (0.616)	1.082 (0.610)	0.064 [−0.148, 0.277], p=0.6
	AD (n=11)	1.122 (0.507)	1.146 (0.524)	0.024 [−0.441, 0.489], p>0.9

*Results with $p < 0.05$ are marked with.

Table 5

Mean (SD) brain atrophy rate (% baseline volume) calculated from baseline and 12-month scans when using piece-wise linear regression (instead of simple linear regression) in the intensity normalisation procedure in KN-BSI, and the difference 95% CI] in mean brain atrophy rate between the consistent and changed acquisitions.

Manufacturer		Consistent acquisition (baseline non-accelerated and repeat non-accelerated scans)	Changed acquisition (baseline non-accelerated and repeat accelerated scans)	Difference (changed - consistent)
GE	**All (n=76)**	**1.063 (0.887)**	**0.663 (0.884)**	**−0.399 [−0.684, −0.114], p=0.006***
	NC (n=20)	0.810 (0.723)	0.480 (0.743)	−0.330 [−0.799, 0.139], p=0.2
	EMCI (n=34)	1.956 (0.738)	0.504 (0.720)	−0.451 [−0.790, −0.113], p=0.01*
	LMCI (n=14)	1.193 (0.917)	0.828 (0.906)	−0.365 [−1.003, 0.302], p=0.3
	AD (n=8)	1.921 (1.326)	1.510 (1.345)	−0.411 [−1.122, 0.301], p=0.2
Philips	**All (n=90)**	**0.762 (0.788)**	**0.722 (0.778)**	**−0.041 [−0.275, 0.194], p=0.7**
	NC (n=25)	0.449 (0.659)	0.368 (0.686)	−0.081 [−0.480, 0.318], p=0.7
	EMCI (n=34)	0.667 (0.622)	0.648 (0.648)	−0.020 [−0.324, 0.285], p=0.9
	LMCI (n=24)	0.891 (0.834)	0.880 (0.768)	−0.011 [−0.440, 0.418], p>0.9
	AD (n=7)	1.900 (0.796)	1.800 (0.714)	−0.0100 [−1.040, 0.841], p=0.8
Siemens	**All (n=256)**	**0.684 (0.768)**	**0.666 (0.780)**	**−0.018 [−0.151, 0.116], p=0.8**
	NC (n=71)	0.541 (0.576)	0.521 (0.623)	−0.020 [−0.198, 0.157], p=0.8
	EMCI (n=118)	0.641 (0.788)	0.611 (0.784)	−0.030 [−0.219, 0.160], p=0.8
	LMCI (n=56)	0.899 (0.914)	0.893 (0.916)	−0.006 [−0.319, 0.307], p>0.9
	AD (n=11)	0.971 (0.579)	1.035 (0.600)	0.064 [−0.417, 0.545], p=0.8

* Results with $p < 0.05$ are marked with.